

CATALYTIC OXIDATION OF 4- HYDROXYBENZOIC ACID ON ACTIVATED CARBON IN BATCH AUTOCLAVE AND FIXED BED REACTOR

*Carmen CREANGA MANOLE, Carine JULCOUR-LEBIGUE**, Anne-Marie WILHELM, Henri
DELMAS

Laboratoire de Génie Chimique de Toulouse (LGC), 5 rue Paulin Talabot BP 1301,

31106 Toulouse Cedex 1, France

*Corresponding author: Carine.Julcour@ensiacet.fr,

tel: +33 (0)5 34 61 52 40, fax: +33 (0) 5 34 61 52 53

Abstract

Catalytic Wet Air Oxidation (CWAO) has been investigated for the treatment of water contaminated by 4-hydroxybenzoic acid (4HBA). Both batch measurements for kinetics determination and continuous trickle bed operation have been performed on the same Activated Carbon (AC). After a fast initial deactivation AC was proved stable and efficient at moderate temperature and oxygen pressure, like for phenol degradation.

The kinetic study in the case of highly adsorbing material as AC may require complex approach to account for the variation of adsorbed reactants during batch oxidation. Adsorption isotherms at reaction temperature and with aged AC have been obtained according to Langmuir equation and used in 4HBA mass balance to derive more significant kinetic parameters. At high catalyst loading and relatively low 4HBA concentration, the variation of 4HBA during the batch oxidation may be even higher on the solid than in the aqueous phase.

Some data in continuous trickle bed reactor or upflow flooded bed reactor indicate a similar oxidation behavior as in batch mode despite very different liquid-solid ratios.

Keywords: catalytic oxidation, 4-hydroxybenzoic acid, kinetics, adsorption, activated carbon

1. Introduction

Aqueous effluents produced by industries or domestic activities often contain organic and especially phenolic compounds in large amounts preventing conventional biological treatment due to their poor biodegradability and even toxicity for the microorganisms.

For rather dilute organic pollutants (for which incineration is too costly or recovery non-profitable), Catalytic Wet Air Oxidation (CWAO) appears as a promising route for pollution abatement and an alternative to other pretreatment processes such as adsorption or non catalytic Wet Oxidation. It avoids the regeneration of adsorbent encountered in adsorption and provides milder operating conditions and more attractive process economics than Wet Air Oxidation.

The major obstacle in its application at industrial scale is the cost and deactivation of the catalyst, which has been subject of numerous studies in the last decades.

Different catalysts have been investigated, based on either noble metals¹⁻⁴ or (mixed) metal oxides^{5,6} with efforts addressed to avoid leaching of the active phase and/or fouling of the catalyst.

Activated Carbon (AC) has recently been successfully applied as a catalyst support by Quintanilla et al.⁷ or even a direct catalyst in CWAO by Fortuny et al.⁸, Eftaxias et al.⁹, Suwanprasop et al.¹⁰ and Santos et al.¹¹ for the destruction of phenol. AC can even perform better than supported catalysts based on the transition metals⁸, probably due to its high adsorption capacity combined to oxygen-containing surface groups. Moreover AC could be thus integrated in a sequential adsorption-regenerative oxidation process¹².

Most of the studies on the CWAO of phenolic compounds have been devoted to phenol itself as model pollutant and only a few papers have investigated the catalytic oxidation of substituted phenols: 2- and 4-chlorophenol and 4-nitrophenol on supported metal oxides^{13,14}, 2-aminophenol, salicylic acid, 5-sulfo salicylic acid, nitrophenols, cresols and chlorophenols on AC¹⁵⁻¹⁷, 2-chlorophenol, 4-coumaric, 4-hydroxyphenylacetic and 4-hydroxybenzoic acids over Pt and Ru supported catalysts¹⁸⁻²¹. Rather different oxidation rates have however been found.

4-hydroxybenzoic acid (4HBA) is of special interest as typically found in wastes of olive oil industry²². It is considered especially toxic and refractory to usual wastewater biological treatment²³. It is also an unexpected intermediate product of phenol oxidation on AC^{9,10}.

This paper deals with CWAO of an aromatic compound, 4-hydroxybenzoic acid, on Active Carbon. The main part of the work is a kinetic analysis based on a new approach with mass balances including variations of the adsorbed reagent. Additional information on intermediate products and on continuous oxidation in fixed bed has been included. Conversely the catalytic aspects and especially tentative explanations of the catalytic performance of AC and the exact nature of deactivation are not presented here. Several papers have been devoted to these questions²⁴, still discussed.

2. Kinetics in batch Autoclave

2.1 Experimental procedure and properties of fresh and aged catalyst

2.1.1 Equipment

For the determination of intrinsic kinetic parameters, batch 4HBA oxidation has been performed in a 300 ml-stirred autoclave (Parr Instruments) shown on Figure 1 and described in details by Suwanprasop²⁵. Operating conditions are: temperature between 130 and 160°C and 1 to 3.5 bar of oxygen partial pressure (total pressure ranging from 10 to 20 bar). 4HBA concentration at the initial time of oxidation is between 2 and 4 g/l.

Kinetic experiments are carried out batchwise for the liquid and continuous for air at a flow rate of 60 l/h (Normal conditions of Temperature and Pressure - NTP) - more than hundred fold oxygen consumption - to ensure a constant oxygen partial pressure despite CO₂ formation. The stirrer speed has been set at 800 rpm such as to avoid on the one hand catalyst attrition and on the other hand eventual external mass transfer limitations of reactants.

Liquid samples have been analyzed by HPLC, using a C₁₈ reverse phase column (ProntoSIL C18 AQ) and a dual wavelength UV detector. Two different methods have been developed: a fast isocratic method, allowing separating 4HBA from other species, and a longer one with graduated elution to separate all intermediates. Only a few samples have been analyzed with the second method.

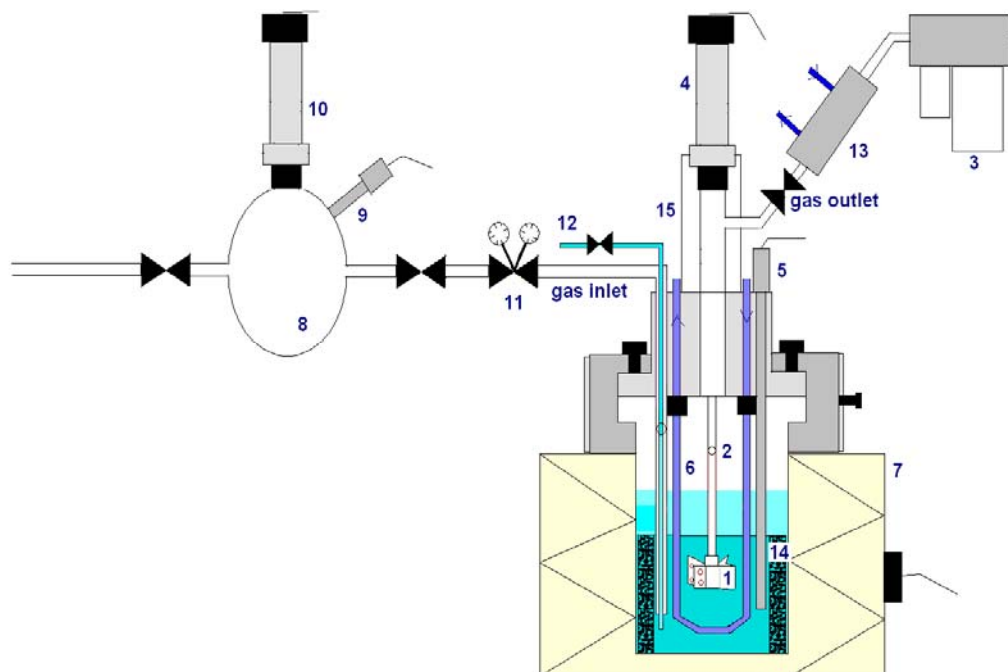


Figure 1. Schema of the autoclave reactor.

1 gas inducing turbine, **2** hollow tube, **3** gas mass-flow controller, **4** pressure transducer, **5** Pt-100 probe, **6** cooling serpentine coil, **7** furnace, **8** gas reservoir, **9** Pt-100 probe, **10** pressure transducer, **11** pressure regulation valve, **12** liquid sampling valve, **13** condenser, **14** catalyst basket, **15** magnetic drive.

2.1.2 Operating protocol

The case of kinetics determination from batch oxidation on activated carbon may require unusual complex procedure due to the need to use large particles undergoing pore diffusion and moreover strong adsorption which should be accounted for in the mass balance.

- Conditioning of the catalyst

Uncrushed Merck AC particles have been sieved to obtain two samples of large particles (1.25-1.6 mm and 0.63-0.8 mm respectively) to minimize fast and continuous deactivation as reported previously during phenol oxidation when using powder²⁶. The properties of the catalyst are listed in Table 1.

Sieved particles size (mm)	1.25 -1.6	0.63-0.8
Volume weighted mean diameter, D[4,3] (mm)[*]	1.25	0.64
Apparent density (g/l)	1032	
Pore volume (cm³/g)	0.57	
BET surface area (m²/g)	980	
Average pore diameter (nm)	22	

Table 1. Physical properties of fresh Merck activated carbon 2514.

^{*}D[4,3] corresponds to the center of gravity of the volume distribution.

The reactor is loaded with 5.3 g of AC particles maintained in a fixed basket and 200 ml of 4HBA solution. As seen in Figure 2, a steep decrease of activity is however observed between the first two runs with particles, but afterwards the time-concentration profiles in the liquid phase are found to be stable for a large number of further experiments as verified with final runs at standard conditions ($p_T=20$ bar, $T=150^\circ\text{C}$). The same largest AC particles (1.25-1.6 mm) are thus used for the entire experimental series to estimate kinetic parameters. The smaller ones are only used for a few runs to investigate pore diffusion effect and derive the pore tortuosity.

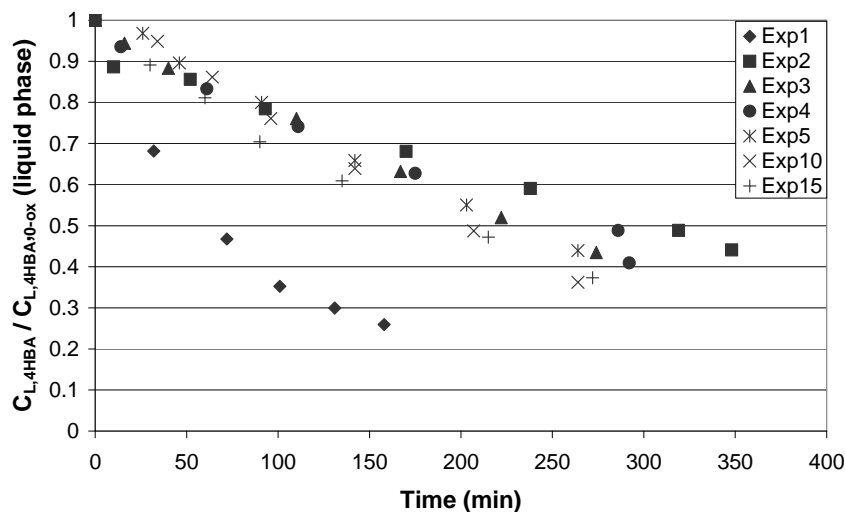


Figure 2. Catalyst stability: time-evolution of 4HBA concentration in the liquid phase (normalized by initial 4HBA concentration). $T=150^{\circ}\text{C}$, $p_{\text{O}_2}=3.2$ bar.

Physical damage of the catalyst due to attrition is not detected. All the withdrawn liquid samples have been found free from suspended fine particles and a granulometry analysis of the used AC shows that the particle size has not changed after reaction experiments.

During the course of reaction, liquid samples have been periodically taken, filtered, and immediately analyzed by HPLC to get the evolution of 4HBA and reaction intermediates.

- Accounting for variations of adsorbed 4HBA during oxidation runs

Activated carbon is known as a very efficient adsorbent. Prior to oxidation runs, AC is saturated with 4HBA under nitrogen at reaction temperature (generally after 2 h) and a liquid sample is taken to measure the initial 4HBA concentration (between 2 and 4 g/l). Then oxygen is provided. During the course of the batch reaction, fast 4HBA adsorption-desorption process occurs driven by liquid-solid equilibrium, and 4HBA concentration decreases in both liquid and solid phases. These two contributions should be summed up at any time to estimate reaction rates from mass balance. The extent of solid phase contribution is much more difficult to quantify accurately, as an important decay of the adsorption capacity of AC particles has been observed, the amount of 4HBA re-adsorbed under nitrogen

prior oxidation being much lower than the value predicted using isotherms with fresh AC. As a consequence adsorption isotherms at reaction temperature and on aged catalyst are to be provided. This is more difficult to obtain than at ambient conditions and on fresh catalyst as it requires to use the autoclave and to achieve a deep preliminary washing out of the many species still adsorbed after several reaction runs.

2.1.3 Characterization of aged AC

- Physical Properties

At the end of the experimental series (16 runs, corresponding to 2.1g of 4HBA treated per g of AC) the analysis of aged AC (Table 2) shows that the BET surface area of AC has decreased from 980 m²/g (for fresh catalyst) to 380 m²/g and pore volume from 0.57 cm³/g to 0.3 cm³/g.

Such a change in AC structure has already been reported during the Catalytic Wet Air Oxidation of phenol and some of its derivatives, attributed to the deposit of high molecular weight organic compounds^{16,17,25}.

In the case of phenol oxidation²⁵, the BET surface area dropped even more to 65 m²/g after treating 1.7g of phenol per g of AC (16 runs).

Volume weighted mean diameter, D[4,3] (mm)	1.25
Apparent density (g/l)	1623
Pore volume (cm³/g)	0.30
BET surface area (m²/g)	380
Average pore diameter (nm)	32

Table 2. Physical properties of aged activated carbon (1.25-1.6 mm sieved fraction).

Thermogravimetric analysis (TGA) of fresh and aged ACs (before washing) has been performed under nitrogen flow from room temperature to 700°C with a heating rate of 10°C/min (Figure 3). It reveals a different behavior of the two catalysts. For the fresh one, weight loss is very small (less than 3%) up to

700°C when decomposition of surface oxygenated groups attached to the AC starts to occur. For the aged one, after water vaporization and release of physisorbed compounds (reactants and intermediates) at temperatures lower than 200°C, significant weight is still observed quite before 700°C, corresponding to the decomposition of chemisorbed species of low volatilities (probably polymers formed by oxidative coupling reactions¹⁶).

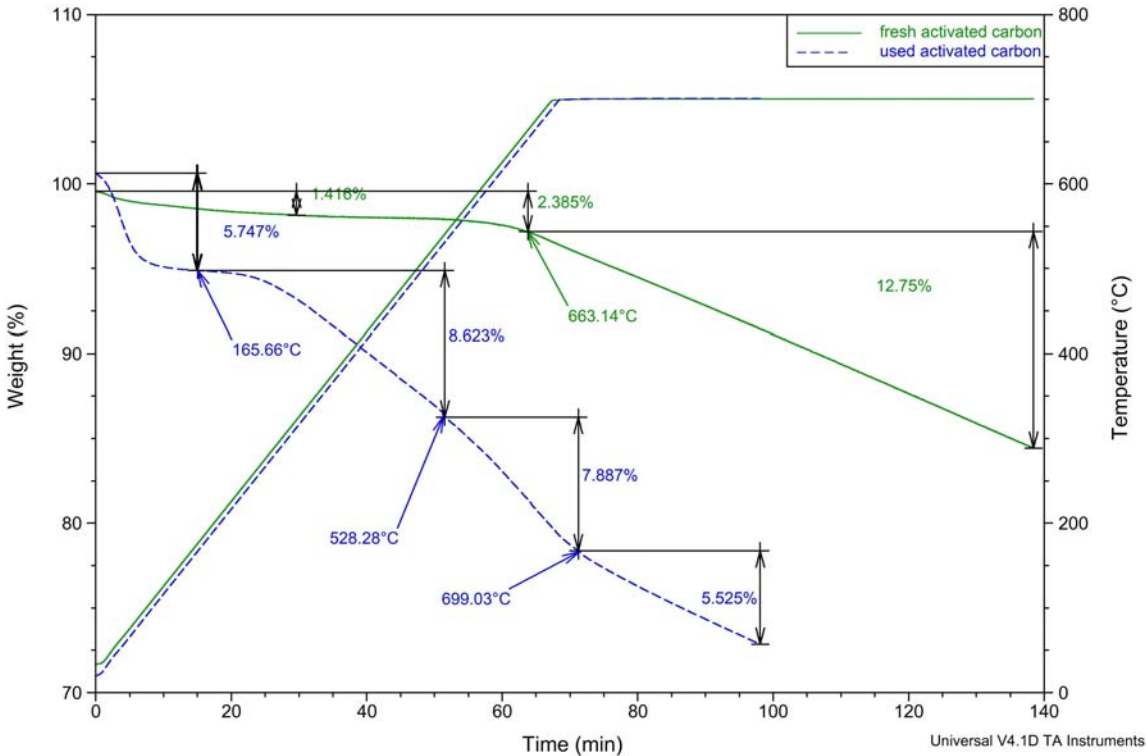


Figure 3. Thermogravimetric analysis of fresh and aged activated carbon.

- Adsorption capacity

After the 4HBA oxidation runs, aged AC particles have been disposed in a fixed bed and washed with bidistilled water during a week so that to eliminate all reversibly-adsorbed components. A batch

desorption of this washed AC has shown that the amount of 4HBA remaining on the solid ($q_0 < 5 \cdot 10^{-5}$ mol/g_{AC}) is then negligible when compared to the saturation value for fresh AC.

After drying, 4HBA adsorption experiments have been then carried out on this aged AC to get the isotherms at both 20°C and 150°C. Isotherms at 20°C have been determined under air atmosphere²⁷, while at 150°C they have been obtained under nitrogen pressure (12 bar) to prevent simultaneous oxidation.

In Figure 4, the corresponding results are compared to those obtained with fresh AC. It is clearly confirmed that the adsorption capacity of aged AC is highly reduced (the saturation value being nearly divided by a factor 2). The isotherm shape is also modified with a quite smoother increase in the low-concentration zone for the aged AC.

Those isotherms are fitted using a Langmuir-type model:

$$q_{4HBA} = q_{\max} \frac{K_{4HBA} C_{4HBA}}{1 + K_{4HBA} C_{4HBA}} \quad (1)$$

The Langmuir parameters, evaluated using linearized equation, are given in Table 3.

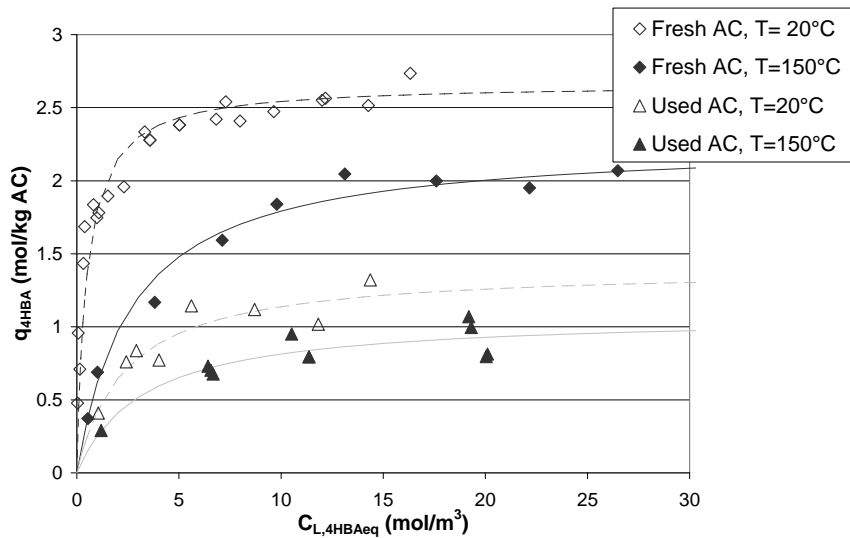


Figure 4. Adsorption isotherms of 4HBA on fresh and aged activated carbon (dots: experimental data, curves: fitted Langmuir models).

	T = 20°C	T = 150°C
Fresh AC	$q_{\max} = 2.66 \text{ mol/kg}_{AC}$ $K_{4HBA} = 2.091 \text{ m}^3/\text{mol}$	$q_{\max} = 2.27 \text{ mol/kg}_{AC}$ $K_{4HBA} = 0.373 \text{ m}^3/\text{mol}$
Aged AC	$q_{\max} = 1.41 \text{ mol/kg}_{AC}$ $K_{4HBA} = 0.424 \text{ m}^3/\text{mol}$	$q_{\max} = 1.08 \text{ mol/kg}_{AC}$ $K_{4HBA} = 0.307 \text{ m}^3/\text{mol}$

Table 3. Langmuir isotherm parameters for 4HBA adsorption on fresh and aged activated carbons.

2.2 Interpretation of reaction data

2.2.1 Oxidation intermediates

When using HPLC gradient method, about ten peaks have been detected, among which nine have been identified: phenol, 2-hydroxybenzoic acid (2HBA), 1,4-benzoquinone, maleic acid, fumaric acid, oxalic acid, formic acid, acetic acid, and malonic acid.

A typical evolution of the concentrations of oxidation intermediates during an experimental run is shown on Figure 5, where concentrations are normalized with respect to the concentration of 4HBA at the initial time of oxidation. As reported in the case of phenol oxidation, formic and acetic acids are the major intermediates^{9,10}, obtained as final organic products derived from oxidative process. The concentrations of other aromatic compounds (especially isomer 2HBA) and other carboxylic acids remain very low.

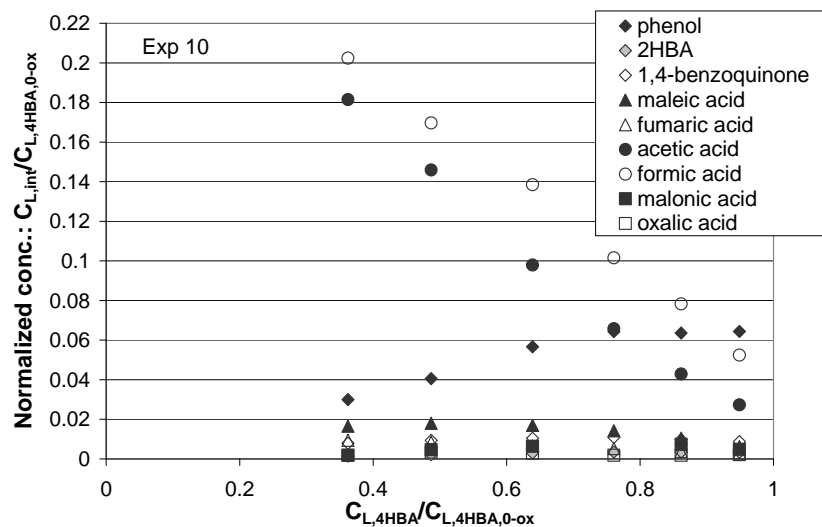


Figure 5. Normalized concentrations of oxidation intermediates as a function of normalized concentration of remaining 4HBA in the liquid phase. $T=150^{\circ}\text{C}$, $p_{\text{O}_2}=3.2$ bar.

In Figure 6, the Chemical Oxygen Demand (COD) calculated from liquid phase concentrations of identified compounds (measured by HPLC) is compared to the COD based on 4HBA only for a few samples from runs 10 to 16. It is shown that those intermediates account for less than 20% of total remaining COD.

From calculations performed on experiment 10, it is shown that at 64% of 4HBA conversion, HPLC-based COD has been reduced by 53%.

Thus, due to the complexity of the reaction system that could involve both diffusion in the catalyst pores, as well as desorption from the solid surface, the kinetic study has been based on the assumption of complete mineralisation of 4HBA in CO_2 and H_2O .

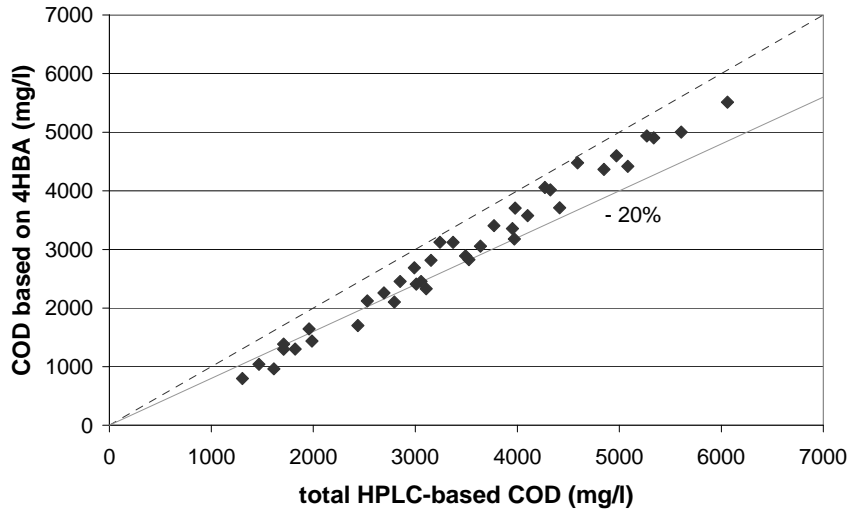


Figure 6. COD based on 4HBA only as a function of COD based on all identified compounds.

2.2.2 Determination of reaction kinetics

Only experiments at stabilized AC activity have been considered to estimate kinetic parameters.

A first order of 4HBA is suggested when plotting the logarithm of 4HBA concentration in the liquid phase as a function of time (not shown here).

Following previous studies of phenol oxidation^{9,28}, a simple power law is then used to describe the 4HBA destruction over AC assuming a first order of 4HBA, while the oxygen order has to be determined by the optimization algorithm.

The following rate equation can thus be proposed:

$$R_{4HBA} = k_0 \exp\left(\frac{-E}{RT}\right) C_{4HBA} x_{O_2}^\alpha \quad (2)$$

A preliminary qualitative analysis of the reaction regime is achieved from an overview of reactions performed with the two particle sizes and two temperatures as presented on Figure 7 where similar behavior at 130°C - corresponding to the kinetic regime, and faster reaction with the smaller particles at 150°C - due to pore diffusion - are observed.

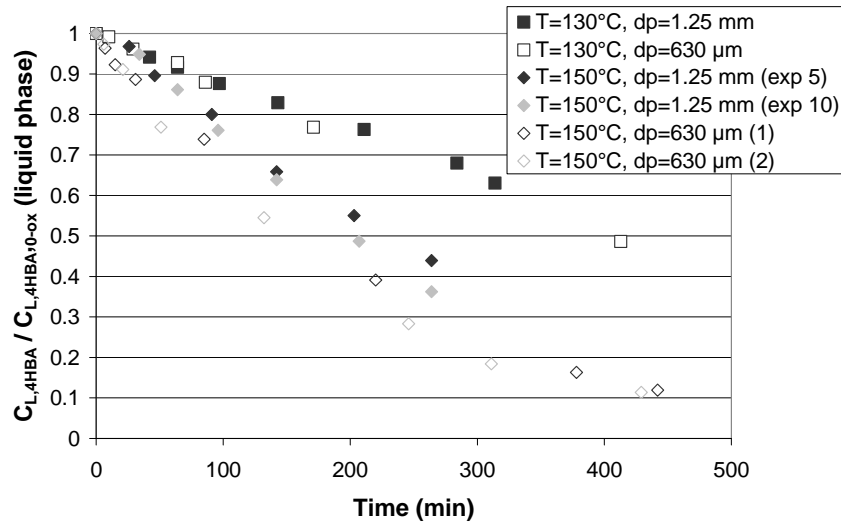


Figure 7. Time-evolution of 4HBA concentration in the liquid phase (normalized by initial 4HBA concentration) for two AC particle sizes. $p_{O_2}=3.2$ bar.

The intrinsic kinetics of 4HBA oxidation has thus to be derived using a batch reactor model that accounts for transient diffusion of both oxygen and 4HBA inside the catalyst pores.

Moreover as mentioned before, 4HBA is present both in the liquid and solid phases, and thus the calculation of reaction rate should account for the total 4HBA disappearance by using adsorption isotherms of aged AC at reaction temperature.

2.2.2.1 Modeling of batch reaction

The proposed model includes transient diffusion of both oxygen and 4HBA inside the catalyst pores, as well as the simultaneous adsorption-desorption on the solid surface.

Model hypothesis

The assumptions are the following ones:

- spherical geometry of particles,
- isothermal particles,
- complete mineralization of reacted 4HBA to CO_2 and H_2O , so that $R_{O_2} = 7 \times R_{4HBA}$,

- negligible external mass-transfer limitation,
- instantaneous adsorption equilibrium,
- no adsorption competition of oxidation intermediates.

Liquid volume variations due to sampling and water vaporization (even limited by the condenser) have been quantified experimentally from the final volume and taken into account in the model.

Model equations

In these conditions, the mass balances lead to the following equations inside the particle:

$$\varepsilon'_p \frac{\partial C_{4HBA}}{\partial t} + \rho'_p \frac{\partial q_{4HBA}}{\partial t} = \frac{D'_{e,4HBA}}{r^2} \frac{\partial}{\partial r} \left(r^2 \frac{\partial C_{4HBA}}{\partial r} \right) - R_{4HBA} \quad (3)$$

$$\varepsilon'_p \frac{\partial C_{O_2}}{\partial t} = \frac{D'_{e,O_2}}{r^2} \frac{\partial}{\partial r} \left(r^2 \frac{\partial C_{O_2}}{\partial r} \right) - 7 \times R_{4HBA} \quad (4)$$

$$q_{4HBA} = q_{\max} \frac{K_{4HBA} C_{4HBA}}{1 + K_{4HBA} C_{4HBA}} \quad (1)$$

with constants given in Table 3 for aged AC at 150°C.

Boundary conditions:

$$\bullet \forall t, r = 0 \quad \frac{\partial C_j}{\partial r} = 0 \quad (\text{condition for symmetry}) \quad (5)$$

$$\bullet \forall t, r = r_p \quad C_j = C_{L,j} \quad (\text{negligible external mass-transfer resistance}) \quad (6)$$

$$\frac{d(V_L \times C_{L,4HBA})}{dt} = -D'_{e,4HBA} \left(\frac{\partial C_{4HBA}}{\partial r} \right)_{r=d_p/2} \frac{W_{AC}}{\rho_p} \frac{6}{d_p} \quad (7)$$

$$C_{L,O_2} = \frac{p_{O_2}}{He} \quad (8)$$

Initial conditions:

$$t=0 \quad C_{4\text{HBA}} = C_{L,4\text{HBA},0-\text{ox}} \quad (\text{after adsorption}) \quad \forall r \quad (9)$$

$$C_{\text{O}_2} = 0 \quad \forall r \quad (10)$$

$$q_{4\text{HBA}} = q_{\text{max}} \frac{K_{4\text{HBA}} C_{4\text{HBA}}}{1 + K_{4\text{HBA}} C_{4\text{HBA}}} \quad (1)$$

ε'_p and ρ'_p are respectively the porosity and apparent density of the aged catalyst particle ($\varepsilon'_p = 0.49$).

ρ_p is the density of the fresh catalyst particle (it has been verified - see Table 2 - that the particle volume is not modified by the carbonaceous deposit).

The effective diffusivity $D'_{e,j}$ is obtained from the molecular diffusivity $D_{m,j}$ (calculated from Wilke-Chang for 4HBA and Diaz et al.²⁹ for O_2):

$$D'_{e,j} = \frac{\varepsilon'_p}{\tau} D_{m,j} \quad (11)$$

with τ the pore tortuosity of the catalyst particles.

Method of resolution

The model leads to a Partial Differential and Algebraic Equations system (PDAE). After normalization, it has been transformed using an orthogonal collocation method for the spatial derivatives³⁰ and the resultant DAE system has been solved using the software DISCo based on the Gear method^{31,32}.

A Gauss-Newton method is applied to optimize from the time-evolution of 4HBA in the liquid phase the oxygen order at 150°C, 1.2 to 3.2 bar of oxygen partial pressure, and the rate constants at different temperatures.

2.2.2.2 Evaluation of model parameters

Due to the complexity of the optimization procedure with many parameters, this optimization has been achieved by steps: first the pore tortuosity involved in the effective diffusivity has been obtained using data corresponding to two particle sizes, then the kinetic parameters at 150°C at which most runs were achieved and finally the activation energy using Arrhenius plot at several temperatures.

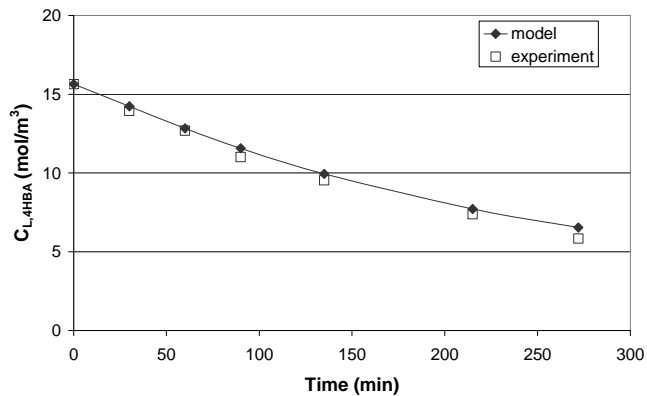
Pore Tortuosity

To get an estimation of the pore tortuosity, some experiments have been carried out with smaller AC particles ($d_p = 630 \mu\text{m}$) in standard conditions ($p_{\text{O}_2}=3.2 \text{ bar}$, $T=150^\circ\text{C}$) up to catalyst activity stabilization and at lower temperature (130°C), using the same amount of catalyst (5.3g). A tortuosity factor $\tau = 3$ has been estimated from these data, in the usual range of tortuosity ($2 \leq \tau \leq 5$).

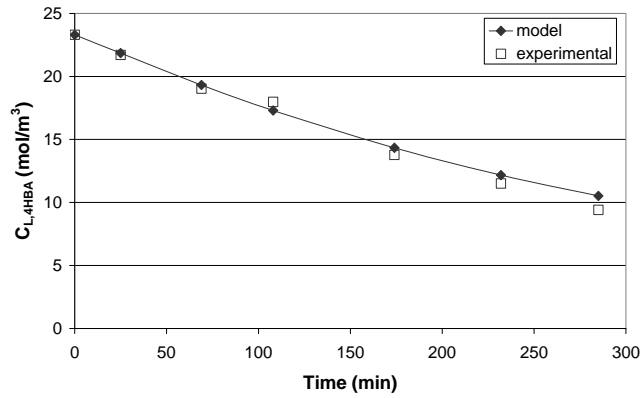
It should be mentioned that higher catalyst loss in the liquid phase has been observed with these smaller particles preventing their use for the complete kinetic study.

Intrinsic kinetic parameters

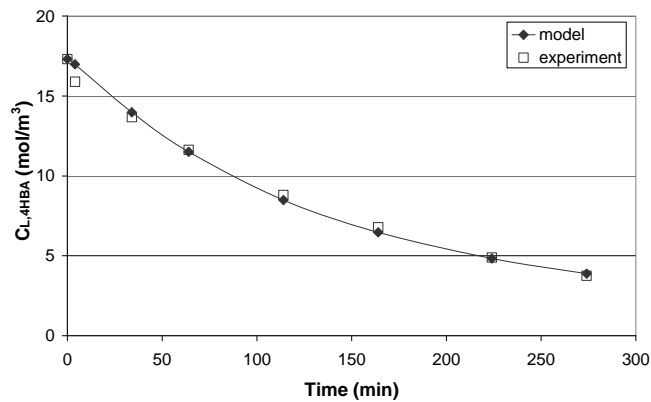
Orders 1 and 0.5 have been checked as possible orders for oxygen resulting from simplification of Langmuir-Hinshelwood type kinetic laws, and a 0.5 oxygen order appears to best fit the 4HBA time-concentration curves (Figure 8). The rate constants optimized at the different temperatures are reported in Table 4.



(a)



(b)



(c)

Figure 8. Experimental and calculated time-concentration profiles in the liquid phase ($W_{cat} = 5.3$ g, stirrer speed of 800 rpm): (a) $p_{O_2} = 3.2$ bar, $T = 150^\circ\text{C}$; (b) $p_{O_2} = 2.2$ bar, $T = 150^\circ\text{C}$; (c) $p_{O_2} = 3.2$ bar, $T = 160^\circ\text{C}$.

Temperature (K)	k (m ³ _L · (m ³ _{AC} · s) ⁻¹)
403	0.18
413	0.33
423	0.81
433	1.85

Table 4. Intrinsic rate constants at different temperatures from batch 4HBA oxidation experiments.

The Arrhenius plot gives activation energy and pre-exponential factor for 4HBA oxidation: 114.6 kJ/mol and $1.167 \times 10^{14} \text{ m}^3_{\text{L}} \cdot (\text{m}^3_{\text{AC}} \cdot \text{s})^{-1}$, respectively.

When not accounting for the evolution of adsorbed 4HBA, the same tortuosity is obtained ($\tau=3$) and the optimization leads to kinetic constants reported in Table 5, resulting in $k_0 = 2.131 \times 10^{10} \text{ m}^3_{\text{L}} \cdot (\text{m}^3_{\text{AC}} \cdot \text{s})^{-1}$ and $E = 86.6 \text{ kJ/mol}$.

Temperature (K)	$k (\text{m}^3_{\text{L}} \cdot (\text{m}^3_{\text{AC}} \cdot \text{s})^{-1})$
403	0.13
413	0.22
423	0.47
433	0.75

Table 5. Intrinsic rate constants at different temperatures from batch 4HBA oxidation experiments, when not accounting for variations of adsorbed 4AHB.

Due to the significant adsorption capacity of AC (even reduced by polymeric deposit) and the operating conditions involving a ratio of liquid to solid volume of only 40, the contribution of the solid phase in 4HBA mass balance is clearly far from being negligible and should be accounted for kinetic optimization.

However these results derived by a rather complex procedure should be even refined by accounting for the possible competitive adsorption of oxidation intermediates.

3. Fixed Bed Reactor

3.1 Experimental set-up and operating conditions

The experimental set-up (Figure 9) detailed in Suwanprasop et al.¹⁰ consists of a jacketed column of 120 cm high and 2.5 cm internal diameter. The reactor is packed with 325 g of activated carbon particles (Merck 2514, 1.25-1.60 mm sieved fraction).

Nine temperature probes and eight sample valves are located at different reactor heights to get axial profiles of temperature and liquid concentrations respectively. Additionally, liquid sampling is done after the gas-liquid separator.

The reactor can operate with either down- or up-flow of gas-liquid according to the position of five three way valves (V1 to V5) located along the gas and liquid circuits. A flexible grid is put at the top of the reactor to prevent fluidization of particles during the upflow operation.

A 2 g/l solution of 4-hydroxybenzoic acid (4HBA) is fed to the column by a dosing pump and the liquid flow rate is checked by measurement of the mass of the feed tank. Gas supply is insured by two mass flow-controllers allowing different gas mixtures.

Temperatures and flow rates are monitored on-line using a data acquisition system implemented in a microcomputer.

The wall temperature is set to 140°C and the total operating pressure to 6 bar. Gas flow rate is 100 l/h (NTP), corresponding to an inlet gas velocity of about 10^{-2} m/s.

By varying the composition of the O₂/N₂ inlet mixture, oxygen partial pressure is adjusted from 0.5 to 2 bar (equilibrium pressure at reactor outlet). Liquid space time (τ_s) varies from 0.1 to 0.7 h (liquid velocities of 0.25 to 1.2 mm/s).

These conditions correspond to the bubble flow regime or transition to pulsed flow regime in upflow mode, and to the trickle flow regime in downflow mode.

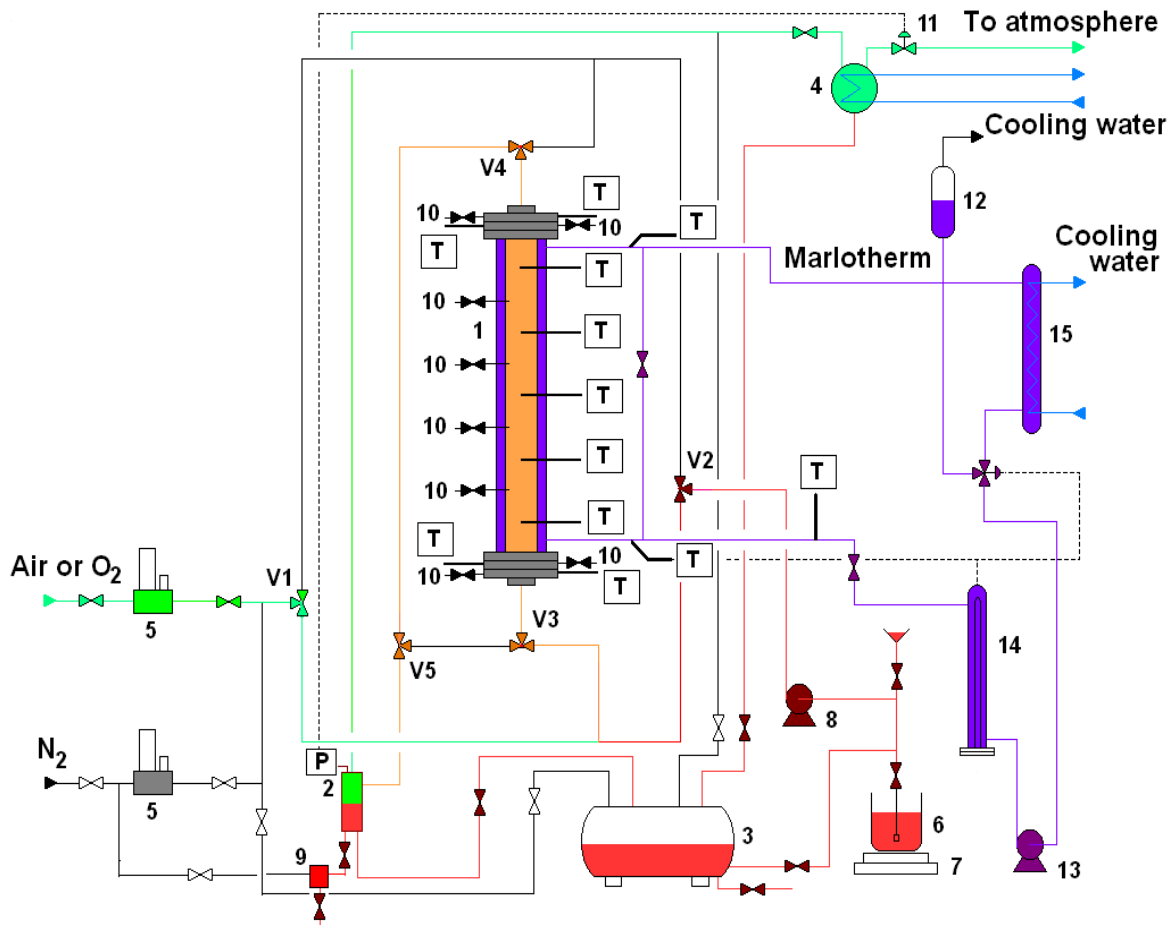


Figure 9. Schematic diagram of cocurrent gas-liquid fixed bed reactor.

1 jacketed packed bed column, 2 gas-liquid separator, 3 liquid storage tank, 4 condenser, 5 gas mass-flow controllers, 6 feed tank, 7 balance, 8 dosing pump, 9 sampling device, 10 liquid sample valves, 11 pneumatic valve, 12 expansion vase, 13 gear pump, 14 heater, 15 cooling exchanger, V1-V5 three-way valves for up- or downflow mode

After packing, the catalyst bed is first saturated with 4HBA at reaction temperature with the 2 g/l solution (under nitrogen flow) until breakthrough is observed at the outlet.

Typical operation of continuous CWAO proceeds then by replacing nitrogen by the O₂/N₂ mixture corresponding to the desired oxygen partial pressure value and setting the selected operating conditions. 4HBA concentration at the reactor outlet has been measured every 30 minutes until steady state of reaction is reached (after 5 to 8 h depending on the operating conditions). At steady state, samples are

collected additionally from every sampling valve along the reactor to get the concentration profiles of 4HBA and reaction products by HPLC.

They are also characterized for the remaining COD according to the closed reflux colorimetric method (Hach spectrophotometer operating at 620 nm).

3.2 Catalytic Wet Air Oxidation of 4HBA

Figure 10 shows the 4HBA conversion versus space-time obtained in upflow operation for $p_{O_2}=2$ bar and conversions obtained at $\tau_s = 0.65$ h for different oxygen partial pressures.

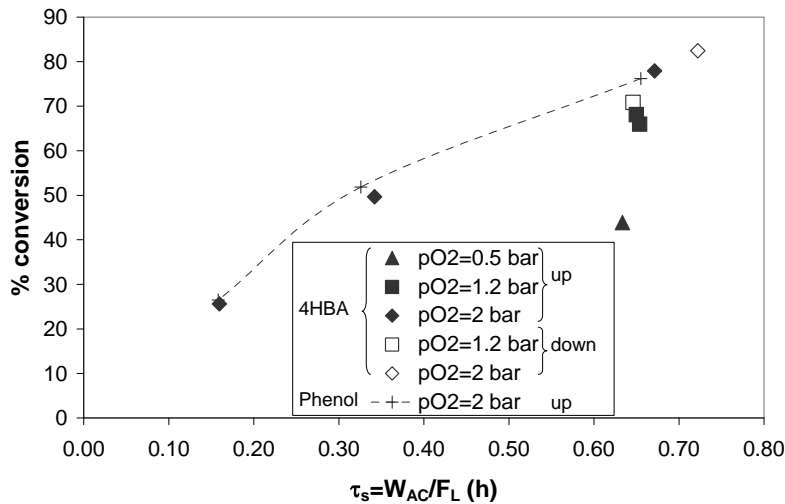


Figure 10. 4HBA and phenol conversions as a function of liquid space-time at different oxygen partial pressures.

As expected, 4HBA destruction improves as pressure and liquid space-time increase. The effect of pressure is however less than that of liquid-space time: multiplying τ_s by a factor 4 results in increasing 4HBA conversion from 26 to 78%, while it increases from 44 to 78% when oxygen pressure is multiplied by 4. This confirms that the order of reaction of oxygen is less than unity, even if the actual

situation is rather complex, involving axial dispersion and water vaporization which can vary noticeably on the liquid flow rate range.

Some experiments have been also carried out in the downflow mode (open symbols in Figure 10), exhibiting similar conversion as in the upflow mode. Such a behavior has also been observed in this pilot reactor for phenol oxidation¹⁰. On the one hand, due to partial wetting of the particles, mass transfer of oxygen to the catalyst is enhanced by direct contacting at the dry solid surface in the trickle flow regime; but on the other hand gas-liquid and liquid-solid mass transfer coefficients are lower in downflow than in upflow mode in those operating conditions.

First and final runs of the experimental series have been carried out in the same operating conditions ($F_L=0.5$ l/h; $p_{O_2}=1.2$ bar) in order to check for catalyst stability. As seen in Figure 10 (filled squares), conversion has remained similar after about 80 working hours (0.4 g of 4HBA treated per g of AC).

Figure 10 also compares the conversions of 4HBA to those obtained in the case of phenol oxidation on AC in the same operating conditions, and shows similar remediation of the two pollutants by the CWAO. Even if feeding concentrations are slightly different (2.43 g/l of phenol and 2 g/l of 4HBA solutions), the results may be compared, as the reaction is first order with respect to the phenolic compound¹⁰. Some authors have tried to correlate the abatement efficiency of the substituted phenols to the electron donating or withdrawing properties of the groups in the aromatic molecule^{16,17}, but actually the oxidation mechanism is rather complex and not fully understood. The comparison is even more difficult as the catalyst undergoes a decrease of its BET surface area that depends on the pollutant (see § 2.1).

3.3 Oxidation intermediates

Figure 11 shows the evolution of the concentration of those intermediates as a function of the remaining 4HBA concentration. To compare their formation rate in the continuous process to that observed in batch conditions (Figure 5), concentrations have been normalized here with respect to the inlet concentration of 4HBA.

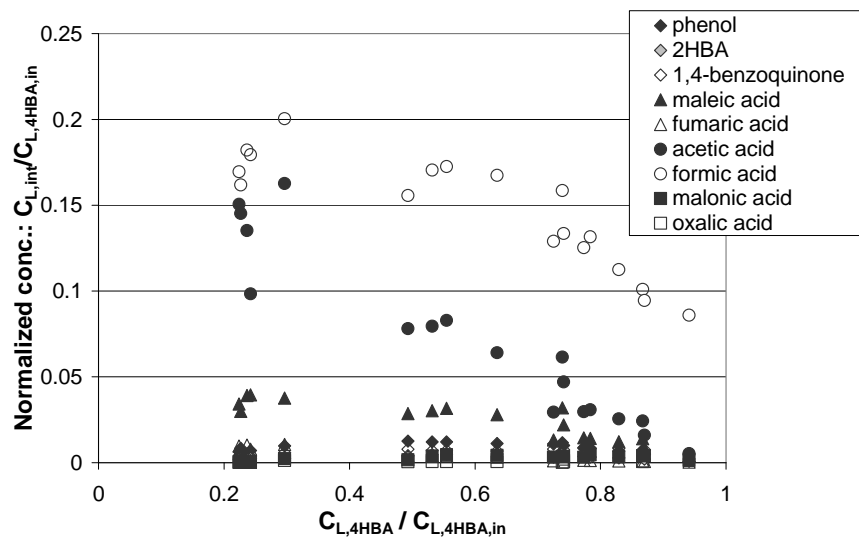


Figure 11. Normalized concentrations of oxidation intermediates as a function of normalized concentration of remaining 4HBA. $T=140^{\circ}\text{C}$, $p_{\text{O}_2}=2$ bar.

The evolution of intermediates concentrations with 4HBA conversion is comparable to that observed in the batch autoclave (Figure 5). Similar values of normalized liquid phase concentrations are also found in both reactors, excepting a higher amount of phenol in the autoclave and of maleic acid in the fixed bed. It can be concluded that oxidation should proceed in the same way in the batch and continuous reactors, despite very different liquid to solid ratios.

Chemical Oxygen Demand (COD) has also been employed in order to evaluate total organic materials in the reaction samples. The comparison of measured COD values (by colorimetric method) and COD values calculated from concentrations of HPLC-identified compounds is presented in Figure 12. As expected, HPLC-based COD values are slightly lower than measured values, but they differ only by about 15%, so that it can be concluded that main reaction intermediates are detected. As in autoclave

reactor and as for phenol degradation, most of the 4HBA consumption results in CO₂ formation, proving AC to be an efficient catalyst for several aromatics degradation.

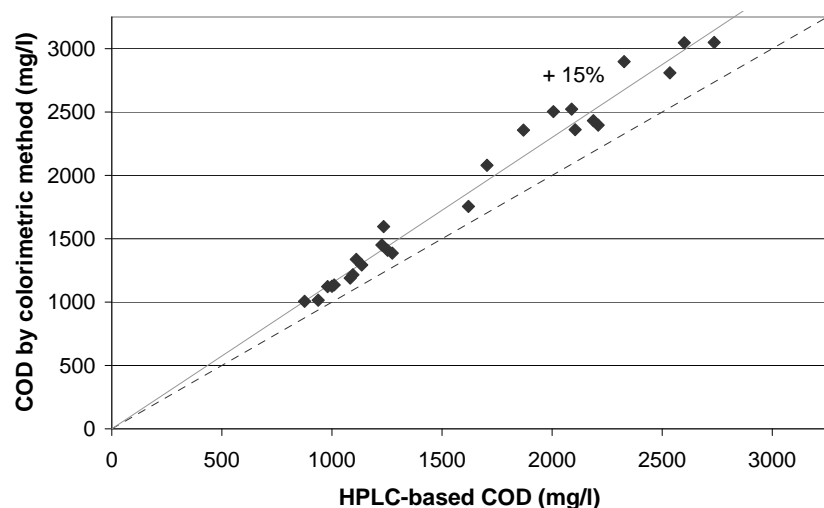


Figure 12. Comparison of measured COD values and HPLC-based COD values.

4. Conclusion

Activated carbon has been used as a catalyst for CWAO of 4-hydroxybenzoic acid solutions both in batch autoclave and in continuous upflow and downflow fixed bed.

Concerning batch experiments for determination of the reaction kinetics, several difficult aspects are to be highlighted.

- First catalyst undergoes a fast initial deactivation, then reaches a steady state, having lost a large fraction of its initial surface area and adsorption capacity.

- Oxidation is not complete as many intermediates appear, most of them being identified as proved by COD comparison. Nevertheless for simplicity, complete mineralisation has been supposed for a kinetic modeling of 4HBA degradation.

- Moreover in the conditions of this work – relatively high catalyst loading and low 4HBA amount – the mass balance on 4HBA during a run should not only use the variation of concentration in liquid phase but also the variation of adsorbed 4HBA on AC. This requires the use of adsorption isotherms on

aged AC at the reaction temperature. It has been shown that this solid content may vary as much as the liquid content, having then a large effect on optimized kinetic parameter values.

Due to this complex and less accurate procedure it is recommended when possible not to carry out kinetic study in such conditions and to verify that adsorption may be neglected in the mass balance.

Concerning continuous fixed bed operation, Activated Carbon performs a satisfactory degradation of this aromatic compound, like phenol, without further observed deactivation and with low aromatic intermediate concentrations. Up to 70% mineralisation is obtained at 80% 4HBA conversion ($p_{O_2}=2$ bar, $T=140^\circ\text{C}$ and $\tau_s=0.7\text{h}$). Further work on complete modeling of upflow flooded bed and downflow trickle bed - including partial wetting - for CWAO is in progress.

Notations

C_j	concentration of compound j (mol/m^3)
$C_{L,j}$	concentration of compound j in the liquid phase (mol/m^3)
$D'_{e,j}$	effective diffusion coefficient of compound j in aged AC pores (m^2/s)
$D_{m,j}$	molecular diffusivity of compound j (m^2/s)
d_p	catalyst particle diameter (m)
E	activation energy (J/mol)
F_L	liquid flow rate (kg/h)
H_e	Henry constant of oxygen in water ($\text{bar} (\text{mol}/\text{m}^3)^{-1}$)
k_0	pre-exponential factor of rate constant in Eq.(1) ($\text{m}^3_L \cdot (\text{m}^3_{AC} \cdot \text{s})^{-1}$)
$K_{4\text{HBA}}$	isotherm constant of 4HBA on AC (m^3/mol)
p_T	total pressure (bar)
p_{O_2}	oxygen partial pressure (bar)
$q_{4\text{HBA}}$	adsorbed amount of 4HBA on activated carbon ($\text{mol}/\text{kg}_{AC}$)
q_{max}	maximum 4HBA adsorption capacity of AC ($\text{mol}/\text{kg}_{AC}$)
r	particle radial coordinate (m)

R	universal gas constant ($8.314 \text{ J kg}^{-1} \text{ K}^{-1}$)
$R_{4\text{HBA}}$	consumption rate of 4HBA ($\text{mol s}^{-1} \text{ m}^{-3}_{\text{AC}}$)
t	time (s)
T	temperature (K)
V_L	liquid volume (m^3)
W_{AC}	catalyst weight (kg)
x	liquid molar fraction

Greek

α	order of reaction of oxygen
ε_p	catalyst porosity
ε_p'	aged catalyst porosity
ρ_p	catalyst particle density (kg/m^3)
ρ_p'	aged catalyst particle density (kg/m^3)
τ	pore tortuosity
τ_s	liquid space time (W_{AC}/F_L) (h)

Subscripts

0-ox	at initial time of oxidation
AC	activated carbon
4HBA	4-hydroxybenzoic acid
in	inlet
int	intermediate
L	liquid
O_2	oxygen
p	particle
T	total

References

- (1) Maugans, C. B. & Akgerman, A. Catalytic wet oxidation of phenol in a trickle bed reactor over a Pt/TiO₂ catalyst. *Wat. Res.* **2003**, *37*, 319.
- (2) Kim, S. K. & Ihm, S. K. Effect of Ce addition and Pt precursor on the activity of Pt/Al₂O₃ catalysts for wet oxidation of phenol. *Ind. Eng. Chem. Res.* **2002**, *41*, 1967.
- (3) Duprez, D.; Delanoë, F.; Barbier Jr. J.; Isnard, P. & Blanchard, G. Catalytic oxidation of organic compounds in aqueous media, *Catal. Today* **1996**, *29*, 317.
- (4) Qin, J.; Zhang, Q. & Chuang, K. T. Catalytic wet oxidation of p-chlorophenol over supported noble metal catalysts, *Appl. Catal. B: Environ.* **2001**, *29*, 115.
- (5) Pintar, A. & Levec, J. Catalytic liquid-phase oxidation of phenol aqueous solutions. A kinetic investigation. *Ind. Eng. Chem. Res.* **1994**, *33*, 3070.
- (6) Hamoudi, S.; Larachi, F. & Sayari, A. Wet oxidation of phenolic solutions over heterogeneous catalysts: degradation profile and catalyst behavior. *J. Catal.* **1998**, *177*, 247.
- (7) Quintanilla, A.; Casas, J. A.; Zazo, J. A.; Mohedano, A. F. & Rodriguez, J. J. Wet air oxidation of phenol at mild conditions with a Fe/activated carbon catalyst. *Appl. Catal. B: Environ.* **2006**, *62*, 115.
- (8) Fortuny, A.; Font, J. & Fabregat, A. Wet air oxidation of phenol using active carbon as catalyst. *Appl. Catal. B: Environ.* **1998**, *19*, 165.
- (9) Eftaxias, A.; Font, J.; Fortuny, A.; Fabregat, A. & Stüber, F. Catalytic wet air oxidation of phenol over active carbon catalyst. Global kinetic modelling using simulated annealing. *Appl. Catal. B: Environ.* **2006**, *67*, 12.
- (10) Suwanprasop, S.; Eftaxias, A.; Stuber, F.; Polaert, I.; Julcour-Lebigue, C. & Delmas, H. Scale up and modelling of fixed bed reactors for the catalytic phenol oxidation over adsorptive active carbon. *Ind. Eng. Chem. Res.* **2005**, *44*, 9513.

- (11) Santos, A.; Yustos, P.; Cordero, T.; Gomis, S.; Rodriguez, S. & Garcia-Ochoa, F. Catalytic wet air oxidation of phenol on active carbon: stability, phenol conversion and mineralization. *Catal. Today* **2005**, *102-103*, 213.
- (12) Polaert, I.; Wilhelm, A. M. & Delmas, H. Phenol wastewater treatment by a two-step adsorption-oxidation process on activated carbon. *Chem. Eng. Sci.* **2002**, *57 (9)*, 1585.
- (13) Pintar, A & Levec, J. Catalytic oxidation of aqueous p-chlorophenol and p-nitrophenol solutions. *Chem. Eng. Sci.* **1994**, *49 (24)*, 4391.
- (14) Posada, D.; Betancourt, P.; Liendo, F. & Brito, J. L. Catalytic wet air oxidation of aqueous solutions of substituted phenols. *Catalysis Letters* **2006**, *106 (1-2)*, 81.
- (15) Tukac, V. & Hanika, J. Catalytic wet oxidation of substituted phenols in the trickle bed reactor. *J. Chem. Technol. Biotechnol.* **1998**, *71*, 262.
- (16) Suarez-Ojeda, M. E.; Stüber, F.; Fortuny, A.; Fabregat, A.; Carrera, J. & Font, J. Catalytic wet air oxidation of substituted phenols using active carbon catalyst. *Appl. Catal. B: Environ.* **2005**, *58*, 105.
- (17) Santos, A.; Yustos, P.; Rodriguez, S. & Garcia-Ochoa, F. Wet oxidation of phenol, cresols and nitrophenols catalyzed by activated carbon in acid and basic media. *Appl. Catal. B: Environ.* **2006**, *65*, 269.
- (18) Kojima, Y.; Fukuta, T.; Yamada, T.; Onyango, M. S.; Bernardo, E. C.; Matsuda, H. & Yagishita, K. Catalytic wet oxidation of o-chlorophenol at mild temperatures under alkaline conditions. *Wat. Res.* **2005**, *39*, 29.
- (19) Li, N.; Descorme, C. & Besson, M. Catalytic wet air oxidation of aqueous solution of 2-chlorophenol over Ru/zirconia catalysts. *Appl. Catal. B: Environ.* **2007**, *71*, 262.

(20) Pham Minh, D.; Gallezot, P. & Besson, M. Degradation of olive oil mill effluents by catalytic wet air oxidation: 1- Reactivity of p-coumaric acid over Pt and Ru catalysts. *Appl. Catal. B: Environ.* **2006**, *63*, 68.

(21) Pham Minh, D.; Aubert, G.; Gallezot, P. & Besson, M. Degradation of olive oil mill effluents by catalytic wet air oxidation: 2-Oxidation of p-hydroxyphenylacetic and p-hydroxybenzoic acids over Pt and Ru supported catalysts. *Appl. Catal. B: Environ.* **2007**, *73*, 236.

(22) Beltran-Heredia, J.; Torregrosa, J.; Dominguez, J. R. & Peres, J. A. Comparison of the degradation of p-hydroxybenzoic acid in aqueous solution by several oxidation processes. *Chemosphere* **2001**, *42*, 351.

(23) Gonzalez, M. D.; Moreno, E.; Quevedo-Sarmiento, J. & Ramos-Cormenzana, A. Studies on antibacterial activity of waste waters from olive oil mills (alpechin): inhibitory activity of phenolic and fatty acids. *Chemosphere* **1990**, *20*, 423.

(24) Stüber, F.; Font, J.; Fortuny, A.; Bengoa, C.; Eftaxias, A. & Fabregat, A. Carbon materials and catalytic wet air oxidation of organic pollutants in wastewater. *Topics in Catalysis* **2005**, *33* (1-4), 3.

(25) Suwanprasop, S. I-Aromatisation of n-hexane and natural gasoline over ZSM-5 zeolite. II-Wet catalytic oxidation of phenol on fixed bed of active carbon. *Ph. D. thesis INP Toulouse, France*, **2005**.
<http://ethesis.inp-toulouse.fr/archive/00000162/>

(26) Stüber, F.; Polaert, I.; Delmas, H.; Font, J.; Fortuny, A. & Fabregat, A. Catalytic wet air oxidation of phenol using active carbon: performance of discontinuous and continuous reactors. *J. Chem. Technol. Biotechnol.* **2001**, *76*, 743.

(27) Andriantsiferana, C.; Manero, M. H.; Fardet-Lemaire, E.; Delmas H. & Wilhelm, A. M. Refractory compounds abatement by adsorption and oxidative catalytic regeneration on activated carbon - Experimental and modelling of competitive adsorption - *1st International Congress on Green Process Engineering* (24-26 April **2007**, Toulouse).

- (28) Fortuny, A.; Bengoa, C.; Font, J.; Castells, F. & Fabregat, A. Water pollution abatement by catalytic wet air oxidation in a trickle bed reactor. *Catal. Today*. **1999**, *53*, 107.
- (29) Diaz, M.; Vega, A. & Coca, J. Correlation for the estimation of gas-liquid diffusivity. *Chem. Eng. Comm.* **1987**, *52*, 271.
- (30) Villadsen, J. V. & Stewart, W. E. Solution of boundary-value problems by orthogonal collocation. *Chem. Eng. Sci.* **1967**, *22*, 1483.
- (31) Hindmarsh, A. C. LSODE and LSODI, two initial value ordinary differential equation solvers. *ACM SIGNUM Newsletter* **1980**, *15* (4), 10.
- (32) Sargousse, A.; Le Lann, J. M.; Joulia, X. & Jourda, L. DISCo: Un nouvel environnement de simulation orienté – objet. *MOSIM'99* (6-8 october **1999**, Annecy), 61 (SCS International).

Acknowledgements

The authors thank Martine Auriol and Christine Rouch from SAP (LGC Toulouse) for physical characterization of the catalyst, Jean-Louis Labat, Lahcen Farhi and Ignace Coghe (LGC Toulouse) for technical assistance and support on the experimental set-ups, Pr. Jean-Marc Le Lann and Dr. Alain Sargousse for their work on DAE solver DISCo.

ANR (Agence Nationale pour la Recherche) and the European Community (under the project Removals-FP6-018525) are gratefully acknowledged for financial support.

LIST OF CAPTIONS:

Figure 1. Schema of the autoclave reactor.

Figure 2. Catalyst stability: time-evolution of 4HBA concentration in the liquid phase (normalized by initial 4HBA concentration). $T=150^{\circ}\text{C}$, $p_{\text{O}_2}=3.2$ bar.

Figure 3. Thermogravimetric analysis of fresh and aged activated carbon.

Figure 4. Adsorption isotherms of 4HBA on fresh and aged activated carbon (dots: experimental data, curves: fitted Langmuir models).

Figure 5. Normalized concentrations of oxidation intermediates as a function of normalized concentration of remaining 4HBA in the liquid phase. $T=150^{\circ}\text{C}$, $p_{\text{O}_2}=3.2$ bar.

Figure 6. COD based on 4HBA only as a function of COD based on all identified compounds.

Figure 7. Time-evolution of 4HBA concentration in the liquid phase (normalized by initial 4HBA concentration) for two AC particle sizes. $p_{\text{O}_2}=3.2$ bar.

Figure 8. Experimental and calculated time-concentration profiles in the liquid phase ($W_{\text{cat}} = 5.3$ g, stirrer speed of 800 rpm): (a) $p_{\text{O}_2} = 3.2$ bar, $T = 150^{\circ}\text{C}$; (b) $p_{\text{O}_2} = 2.2$ bar, $T = 150^{\circ}\text{C}$; (c) $p_{\text{O}_2} = 3.2$ bar, $T = 160^{\circ}\text{C}$.

Figure 9. Schematic diagram of cocurrent gas-liquid fixed bed reactor.

Figure 10. 4HBA and phenol conversions as a function of liquid space-time at different oxygen partial pressures.

Figure 11. Normalized concentrations of oxidation intermediates as a function of normalized concentration of remaining 4HBA. $T=140^{\circ}\text{C}$, $p_{\text{O}_2}=2$ bar.

Figure 12. Comparison of measured COD values and HPLC-based COD values.